Contribution of Chain Termini to the Conformational Stability and Biological Activity of Onconase†

Eugenio Notomista,‡ Francesca Catanzano,§ Giuseppe Graziano,|| Sonia Di Gaetano,‡ Guido Barone,⊥ and Alberto Di Donato*,‡

Dipartimento di Chimica Biologica, Università di Napoli Federico II, Via Mezzocannone, 16-80134 Napoli, Facoltà di Scienze Ambientali, Seconda Università di Napoli, Via Vivaldi, 81100 Caserta, Facoltà di Scienze, Università del Sannio, Via Port'Arsa, 11-82100 Benevento, and Dipartimento di Chimica, Università di Napoli Federico II, Via Cinthia, 45-80126 Napoli, Italy

Received April 12, 2001; Revised Manuscript Received May 25, 2001

ABSTRACT: Onconase, a member of the RNase A superfamily, is a potent antitumor agent which is undergoing phase III clinical trials as an antitumor drug. We have recently shown that onconase is an unusually stable protein. Furthermore, the protein is resistant to the action of proteases, which could influence its use as a drug, prolonging its biological life, and leading to its renal toxicity. Our investigation focused on the contribution of chain termini to onconase conformational stability and biological activities. We used differential scanning calorimetry, isothermal unfolding experiments, limited proteolysis, and catalytic and antitumor activity determinations to investigate the effect of the elimination of the two blocks at the chain termini, the N-terminal cyclized glutamine and the C-terminal disulfide bridge between the terminal Cys104 and Cys87. The determination of the thermodynamic parameters of the protein led to the conclusion that the two blocks at onconase chain termini are responsible for the unusual stability of the protein. Moreover, the reduced stability of the onconase mutants does not influence greatly their catalytic and antitumor activities. Thus, our data would suggest that an onconase-based drug, with a decreased toxicity, could be obtained through the use of less stable onconase variants.

Onconase (ONC)[1] is a small ribonuclease found in the eggs of the leopard frog (*Rana pipiens*) (*1*). It belongs to the RNase A superfamily, and shares with RNase A ~30% sequence identity and a very similar fold, even though it is 20 residues shorter (*2*). Its structure consists of two β-sheets and three α-helices; helices α2 and α3 shield from water the two β-sheets that form the characteristic V-shaped motif, in the middle of which helix α1 is positioned (Figure 1). As a biomolecule, ONC possesses several peculiarities: it exhibits antitumor and antiviral activities (*3*), and is resistant to the cytosolic ribonuclease inhibitor (*4*, *5*). As a potential antitumor drug, ONC has already reached phase III clinical trials (*6*). In addition, we have recently shown that ONC is an unusually stable protein as indicated by its high denaturation temperature, 89 °C pH 6, and its resistance to guanidinium chloride (GuHCl) and to proteases (*7*).

Thus, ONC is an attractive model for studying the molecular determinants of protein stability and their influence on its biological properties. Furthermore, ONC stability, especially its resistance to proteases, could influence its use as a therapeutic agent. In fact, resistance to degradation could prolong its biological life. However, it should be taken into account that an excessive stability could lead to increased toxicity. Indeed, it has been demonstrated that ONC accumulates in the kidney (*8*) and that its main form of toxicity is renal (*9*).

A specific structural feature of ONC is the tight anchoring of both its chain termini to the body of the molecule. The N-terminal glutamine of ONC cyclizes to form a pyroglutamyl residue that is H-bonded to the ϵ-amino group of the Lys9 side chain, and to the CO group of Val96, via the NH group of the cyclic amide. Also, the C-terminus is blocked by a disulfide bridge between the terminal Cys104 and Cys87. This bridge should make an important contribution to the conformational stability of the native structure anchoring the C-terminus to one of the two β-sheets of ONC.

To assess the contribution of chain termini to ONC conformational stability and biological activities, we have prepared mutants in which the two blocks at the chain termini

† This work was supported by grants from the Ministry of University and Research (PRIN/97, SMIP, and PRIN/97, CFSIB), the MURST-CNR Program L. 95/95, and the National Research Council (PF-Biotecnologie).

* To whom correspondence should be addressed. Telephone: +39-081-2534 734. Fax: +39-081-552 1217. E-mail: didonato@unina.it.

‡ Dipartimento di Chimica Biologica, Università di Napoli Federico II.

§ Seconda Università di Napoli.

|| Università del Sannio.

⊥ Dipartimento di Chimica, Università di Napoli Federico II.

[1] Abbreviations: ONC, onconase; RNase A, bovine pancreatic ribonuclease A; (C87S, des104)-ONC, mutant of onconase with serine replacing cysteine at position 87 and with deletion of Cys104; (C87S, des103−104)-ONC, mutant of onconase with serine replacing cysteine at position 87 and with deletion of Ser103 and Cys104; Met(−1)-ONC, onconase variant with a metionine residue preceding Gln1; (Q1E)-ONC, mutant of onconase with glutamic acid replacing glutamine at position 1; ES/MS, electrospray mass spectrometry; DSC, differential scanning calorimetry; MES, 2-(*N*-morpholino)ethanesulfonic acid; HEPPSO, *N*-(2-hydroxyethyl)piperazine-*N*′-2-hydroxypropanesulfonic acid; Tris, tris(hydroxymethyl)aminomethane; GuHCl, guanidinium chloride; RP-HPLC, reverse-phase high-performance liquid chromatography; PDB, Protein Data Bank.

10.1021/bi010741s CCC: $20.00
Published on Web 07/12/2001

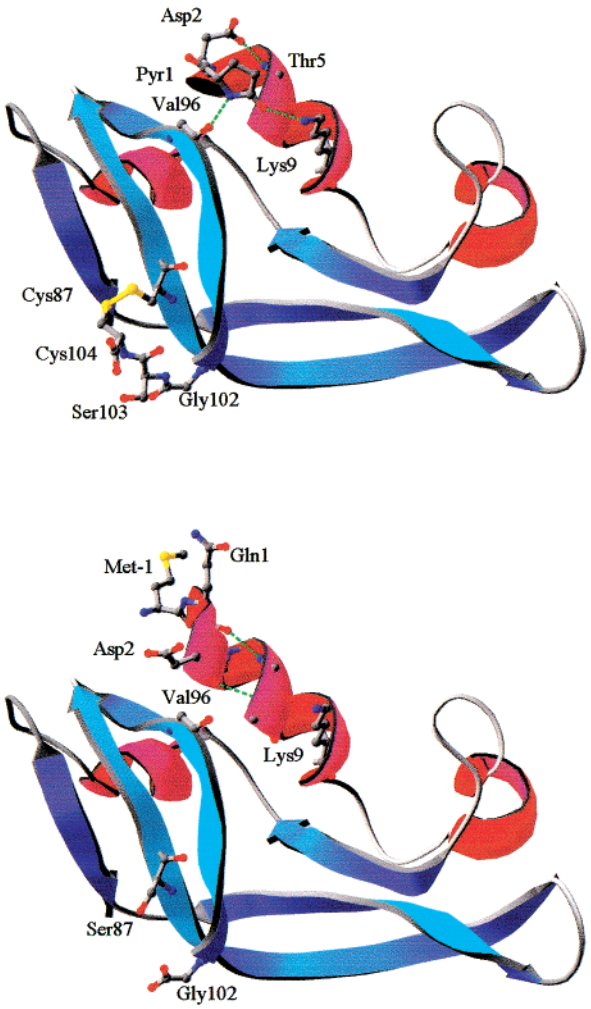

FIGURE 1: (Top) Crystal structure of ONC (PDB entry 1ONC). (Bottom) Structural model of Met(−1)-(C87S, des103−104)-ONC. Helices are colored in red and β-strands in light blue. Residues of the active sites and at chain termini are colored according to the following codes: carbons, gray; nitrogens, blue; oxygens, red; and sulfurs, yellow. Green dotted lines represent H-bonds.

have been eliminated. We produced a recombinant ONC form retaining the N-terminal Met(−1), which was thus unable to produce a blocked amino terminus through cyclization of Gln1, denoted Met(−1)-ONC. As for the C-terminal disulfide bridge, we removed Cys104 and replaced Cys87 with a serine residue. This mutant was denoted (C87S, des104)-ONC. In addition, we prepared mutant (C87S, des103−104)-ONC by removing both Ala103 and Cys104 and mutant Met(−1)-(C87S, des103−104)-ONC, in which both blocks at the chain termini have been eliminated. Differential scanning calorimetry (DSC) and fluorescence measurements were performed to investigate the stability of the ONC variants as a function of temperature and GuHCl. The proteins were also probed for their susceptibility to pepsin. Finally, the ribonuclease and antitumor activities of the mutants were determined.

MATERIALS AND METHODS

Materials. Plasmid pET22b(+) and *Escherichia coli* strain BL21(DE3) were from AMS Biotechnology. *E. coli* strain JM101 was purchased from Boehringer, and labeled oligonucleotides were from Amersham. The Wizard DNA purification kit for elution of DNA fragments from an agarose gel, enzymes, and other reagents for DNA manipulation were from Promega.

General Procedures. Bacterial cultures, plasmid purifications, and transformations were performed according to the methods of Sambrook et al. (*10*). Double-stranded DNA was sequenced with the dideoxy method of Sanger et al. (*11*), carried out with a Sequenase version II kit (Amersham) with deoxynucleotide triphosphates purchased from Pharmacia.

Recombinant Protein Expression and Purification. The cDNA encoding Met(−1)-ONC cloned between *Nde*I and *Bam*HI sites of vector pET22b(+) was produced as described previously (*7*). This cDNA was further mutated using oligonucleotide-mediated site-directed mutagenesis according to the method of Kunkel (*12*) to replace the cysteine residue at position 87 with serine and to delete residue Cys104 or residues Ser103 and Cys104, yielding the coding sequence for mutants (C87S, des104)-ONC and (C87S, des103−104)-ONC, respectively. All the proteins were expressed and purified as described previously (*13*), with an average yield of ∼35−40 mg of protein per liter of bacterial culture. The Met(−1) variants were purified by omitting the digestion with *Aeromonas proteolytica* aminopeptidase (*13*). Recombinant ONC and the mutants were characterized by N-terminal sequencing and by determination of their molecular weight by ES/MS. Protein preparations were routinely checked for contamination by higher-molecular weight ribonucleases by SDS−PAGE followed by activity staining (*14*).

Scanning Calorimetry. DSC measurements, buffers, sample handling, and data treatment were carried out as described previously (*7*). Briefly, the excess heat capacity function $\langle \Delta C_p \rangle$ was obtained after baseline subtraction, assuming that the baseline is given by the linear temperature dependence of the native state heat capacity (*15*), and the calorimetric enthalpy $\Delta_d H(T_d)$ was determined by direct integration of the area under the curve. The van't Hoff enthalpy was calculated with the formula (*16*)

$$\Delta_d H_{vH}(T_d) = 4RT_d^2[\langle \Delta C_p(T_d) \rangle / \Delta_d H(T_d)] \qquad (1)$$

where T_d is the denaturation temperature and corresponds to the maximum of the DSC peak, $\langle \Delta C_p(T_d) \rangle$ is the value of the excess molar heat capacity function at T_d, and R is the gas constant. The closeness to 1 of the cooperative unit [CU $= \Delta_d H(T_d)/\Delta_d H_{vH}(T_d)$] is necessary for the denaturation to be a two-state transition (*16*, *17*).

Buffers were purchased from Sigma and included glycine-HCl, acetic acid/sodium acetate, MES, and HEPPSO. Protein concentrations were determined spectrophotometrically using an ϵ_{280} of 10 400 M^{-1} cm^{-1} for all the proteins.

GuHCl-Induced Denaturation. GuHCl-induced denaturation experiments were monitored by fluorescence emission and carried out as described previously (*7*).

The two-state N ⇔ D transition model was used to analyze the denaturation curves. The modified linear extrapolation model (LEM) (*18*) was used, assuming a linear variation of $\Delta_d G$ with denaturant concentration:

$$\Delta_d G = \Delta_d G_{H_2O} - mc_{GuHCl} \qquad (2)$$

where $\Delta_d G_{H_2O}$ is the value of $\Delta_d G$ in the absence of GuHCl

and m is a measure of the dependence of $\Delta_d G$ on GuHCl concentration. Furthermore, $\Delta_d G_{H_2O} = m(c_{GuHCl})_{1/2}$, where $(c_{GuHCl})_{1/2}$ represents the midpoint of the denaturation region. Also, the spectroscopic signals of native (Y_N) and denatured (Y_D) states are assumed to vary linearly with GuHCl concentration, following the equation $Y_i = a_i + b_i c_{GuHCl}$. Under these assumptions, the observed spectroscopic signal is given by

$$Y = \{Y_N + Y_D \exp[-(\Delta_d G_{H_2O} - mc_{GuHCl})/RT]\}/\{1 + \exp[-(\Delta_d G_{H_2O} - mc_{GuHCl})/RT]\} \quad (3)$$

A nonlinear least-squares regression was carried out to estimate the unknown parameters associated with the conformational transition, according to the minimum χ^2 value. The nonlinear regression using the Levenberg−Marquardt algorithm was performed as implemented in the Optimization Toolbox of MATLAB.

Proteolysis Experiments. ONC and its variants, at 0.8 mg/mL, were treated with pepsin at a pepsin:ribonuclease ratio of 1:10 (w:w), in 50 mM glycine-HCl, at pH 2.4 and 30 °C. Aliquots of the reaction mixture were withdrawn at suitable time intervals, and the reaction was stopped by increasing the solution pH to 8.0 by adding Tris. Then, 2-mercaptoethanol and SDS were added up to final concentrations of 20 mM and 0.1% (w:v), respectively. After 5 min at 100 °C, samples were analyzed by SDS−PAGE (*19*), and Coomassie-stained bands were quantified by densitometry.

Protein Modeling. The programs Swiss-PDB-Viewer (*20*) and InsightII (MSI, San Diego, CA) were used to inspect protein structures and to build models of ONC variants.

Cell Cultures. Human chronic myelogenous leukemia K562 cells, malignant SV40-transformed SVT2 fibroblasts, and the parental nontransformed Balb/C 3T3 line were obtained from ATCC (Richmond, VA), and cultured in 24-well plates at a density of 50×10^3 cells/mL of Dulbecco's modified Eagle's medium, supplemented with glutamine, penicillin, streptomycin, and 10% fetal calf serum. The proteins that were being tested were added to the cells before plating, and cells were counted after 48 h.

Other Methods. Protein sequence determinations were performed on an Applied Biosystems (Foster City, CA) sequenator (model 473A), connected on-line with a high-performance liquid chromatography apparatus for identification of phenylthiohydantoins. SDS−PAGE was carried out according to the method of Laemmli (*21*). RNase activity on yeast RNA was assayed with the method of Kunitz (*22*). The electrospray mass spectrometric (ES/MS) analyses were performed using an Api-100 triple-quadrupole mass spectrometer (Perkin-Elmer) equipped with an electrospray ion source, at CEINGE Biotecnologie Avanzate (Naples, Italy).

RESULTS

Temperature-Induced Denaturation. The thermal stability of ONC and its mutant forms was studied by means of DSC measurements in the pH range of 2.0−8.0 in 100 mM buffer. The thermal denaturation proved to be reversible for all the proteins, with the exception of the experiments at pH 8.0, as judged by the reheating criterion. The thermodynamic parameters that were obtained are reported in Table 1, and representative DSC curves are shown in Figure 2. In all cases, the values of the cooperative unit (CU) are close to 1; hence, for all the proteins that were tested, the process is well represented by the two-state N ⇔ D transition model.

Table 1: Thermodynamic Parameters of the Temperature-Induced Denaturation of ONC and Some Mutant Forms at Different pH Values Obtained from DSC Measurements[a]

	pH	T_d (°C)	$\Delta_d H(T_d)$ (kJ/mol)	$\Delta_d C_p$ (kJ K^{-1} mol^{-1})	CU
ONC	2.0	69.5	425	6.2	0.97
(104 aa)	4.0	86.8	525	5.2	0.99
	6.0	88.7	540	5.5	1.01
	8.0	85.4	515	5.8	0.97
Met(−1)-ONC	2.0	64.3	395	5.3	0.98
(105 aa)	4.0	81.6	490	6.0	1.03
	6.0	84.0	505	5.7	0.98
	8.0	79.7	470	4.9	1.02
(C87S,	2.0	43.2	255	5.4	1.03
des104)-ONC	4.0	65.5	370	5.6	0.99
(103 aa)	6.0	70.2	405	5.2	1.02
	8.0	67.8	380	6.0	0.96
(C87S,	2.0	43.0	245	5.1	0.97
des103−104)-ONC	4.0	65.0	370	6.2	1.04
(102 aa)	6.0	69.3	400	5.8	1.01
	8.0	67.0	380	6.0	0.95
Met(−1)-(C87S,	2.0	38.8	210	4.9	1.06
des103−104)-ONC	4.0	60.3	340	5.8	1.01
(103 aa)	6.0	64.0	365	5.4	0.97
	8.0	61.8	345	6.3	1.02

[a] CU is the cooperative unit given by the calorimetric to van't Hoff enthalpy ratio, calculated at the denaturation temperature. Each value is the mean value of four measurements. The error in T_d does not exceed 0.2 °C. The errors for $\Delta_d H(T_d)$ and $\Delta_d C_p$ amount to 5 and 10%, respectively, of the reported values. The data for ONC are from ref *7*. aa, amino acids.

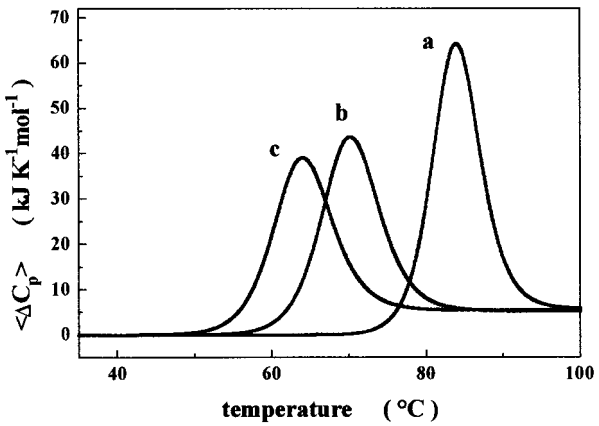

FIGURE 2: DSC profiles at pH 6.0 with 100 mM MES buffer: (a) Met(−1)-ONC, (b) (C87S, des104)-ONC, and (c) Met(−1)-(C87S, des103−104)-ONC.

A comparison of the experimental data collected on wild-type ONC and on its variants (see Table 1) indicates that the elimination of the two blocks at the chain termini causes a significant decrease in the thermal stability of the ONC folded structure. At pH 6.0, 100 mM MES buffer, where the five proteins show the maximal thermal stability, ONC has a T_d of 88.7 °C and a $\Delta_d H(T_d)$ of 540 kJ/mol, whereas Met(−1)-ONC has a T_d of 84.0 °C and a $\Delta_d H(T_d)$ of 505 kJ/mol. The removal of the C-terminal disulfide bridge has a more pronounced effect. (C87S, des104)-ONC has a T_d of 70.2 °C and a $\Delta_d H(T_d)$ of 405 kJ/mol, whereas (C87S, des103−104)-ONC has a T_d of 69.3 °C and a $\Delta_d H(T_d)$ of 400 kJ/mol. Finally, Met(−1)-(C87S, des103−104)-ONC, the mutant lacking both blocks at the N- and C-termini, has

Table 2: Thermodynamic Parameters of the GuHCl-Induced Denaturation, at 25 °C and pH 6.0 with 100 mM MES Buffer, of ONC and Its Mutants, Recorded by Monitoring the Shift in the Fluorescence Maximum Wavelength[a]

	$(c_{GuHCl})_{1/2}$ (M)	m (kJ mol^{-1} M^{-1})	$\Delta_dG_{H_2O}$ (kJmol)	Δ_dG(25 °C) (kJ/mol)
ONC	4.5	12.9 ± 0.8	58.0 ± 2.5	59
Met(−1)-ONC	4.3	12.6 ± 0.9	54.0 ± 3.0	55
(C87S, des104)-ONC	2.9	13.0 ± 1.0	37.8 ± 2.6	36
(C87S, des103−104)-ONC	2.8	12.8 ± 1.0	36.0 ± 2.8	35
Met(−1)-(C87S, des103−104)-ONC	2.3	12.3 ± 1.2	28.3 ± 3.0	30

[a] The reported values are the results of nonlinear least-squares regressions of λ_{max} vs c_{GuHCl} plots. $(c_{GuHCl})_{1/2} = \Delta_dG_{H_2O}/m$ is the midpoint of the GuHCl denaturation curve. The values of Δ_dG(25 °C) are calculated by means of the Gibbs−Helmholtz relationship, using the parameters determined in DSC measurements. Reported errors are the standard deviations of nonlinear regressions. The data for ONC are from ref *7*.

a T_d of 64.0 °C and a $\Delta_dH(T_d)$ of 365 kJ/mol. Thus, elimination of both blocks at the chain termini leads to a very significant decrease in the denaturation temperature of ∼25 °C.

It should be noted that the mutant Met(−1)-(C87S, des103−104)-ONC has a thermal stability similar to that of RNase A, the obvious standard for members of the ribonuclease superfamily, which exhibits, under the same experimental conditions, a T_d of 62.4 °C, a $\Delta_dH(T_d)$ of 470 kJ/mol, a Δ_dC_p of 5.8 kJ K^{-1} mol^{-1}, and a CU of 1.02 (*23*, *24*).

It should also be noted that the elimination of the blocks at the two chain termini has additive effects on the decrease in the denaturation temperature. In fact, a ΔT_d of −24.7 °C is found for Met(−1)-(C87S, des103−104)-ONC, whereas the ΔT_d values are −4.7 °C for Met(−1)-ONC and −19.4 °C for (C87S, des103−104)-ONC. This finding is not surprising, as the chain termini are not very close in space, so the two perturbations introduced by the mutations can be considered independent from each other. It is evident that the removal of the C-terminal disulfide bridge causes a significant reduction in the denaturation enthalpy change. This is an indication of the loss or weakening of inter-residue attractive interactions.

GuHCl-Induced Denaturation. To further characterize the stability of the mutants, GuHCl-induced denaturation curves were recorded at 25 °C and pH 6.0 in 100 mM MES buffer, using as a probe the shift in fluorescence maximum wavelength upon excitation at 280 nm. For all the proteins that were tested, the fluorescence maximum wavelength upon denaturation undergoes an abrupt change from 326 to 351 nm. This red shift is mainly due to water exposure of the Trp3 side chain, which in the folded conformation is buried in a hydrophobic pocket lined by the nonpolar moieties of the Phe6, Gln7, Pro41, Lys45, and Pro95 side chains.

All GuHCl-induced denaturation experiments proved to be reversible; hence, the experimental curves were analyzed by the two-state N ⇔ D transition model. The values of m, $\Delta_dG_{H_2O}$, and $(c_{GuHCl})_{1/2}$ obtained from the nonlinear regressions are listed in Table 2, while representative curves are shown in Figure 3. The experimental results lead us to conclude that the mutant forms of ONC are less stable than the parent enzyme, as indicated by the $(c_{GuHCl})_{1/2}$ and $\Delta_dG_{H_2O}$ values. It is noteworthy that the $\Delta_dG_{H_2O}$ values agree, within experimental error, with those calculated by means of the Gibbs−Helmholtz relationship, using the parameters determined in the DSC measurements, and reported in the fifth column of Table 2.

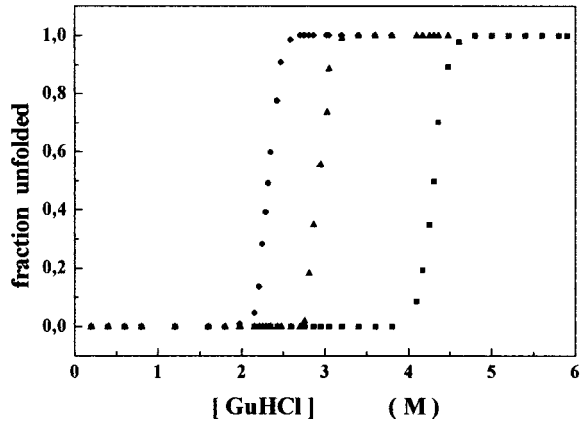

FIGURE 3: GuHCl denaturation curves recorded by monitoring the shift in the fluorescence maximum wavelength with 100 mM MES buffer at pH 6.0 and 25 °C: Met(−1)-ONC (■), (C87S, des104)-ONC (▲), and Met(−1)-(C87S, des103−104)-ONC (●).

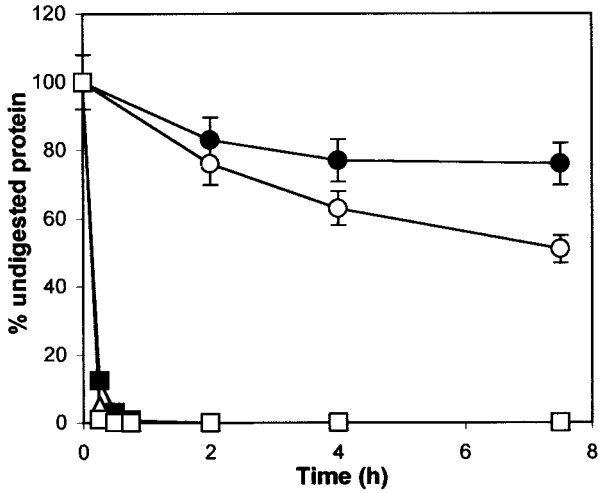

FIGURE 4: Densitometric curves of proteolytic digestion by pepsin of ONC (●), Met(−1)-ONC (○), (C87S, des104)-ONC (△), (C87S, des103−104)-ONC (■), and Met(−1)-(C87S, des103−104)-ONC (□). The curves were obtained as described in Materials and Methods. Standard errors are shown for only ONC and Met(−1)-ONC.

Finally, the estimates of parameter m are very close for the five proteins. Since m is a measure of the cooperativity of the unfolding transition, this would indicate that there are no differences in cooperativity between the variant forms that were investigated, in agreement with the DSC results.

Proteolysis Experiments. ONC is particularly resistant to pepsin, and we have already suggested that both the high denaturation temperature and the resistance to proteases could be an indication of its structural rigidity (*7*). To test if the chain termini of ONC contribute to its resistance to proteolysis, ONC mutants were treated with pepsin (see Figure 4). As previously reported (*7*), only 20% of ONC was degraded after treatment for 8 h, whereas Met(−1)-ONC is more prone to pepsin attack as ∼50% of the protein was digested under the same conditions. On the other hand, the removal of the C-terminal disulfide bridge has a dramatic

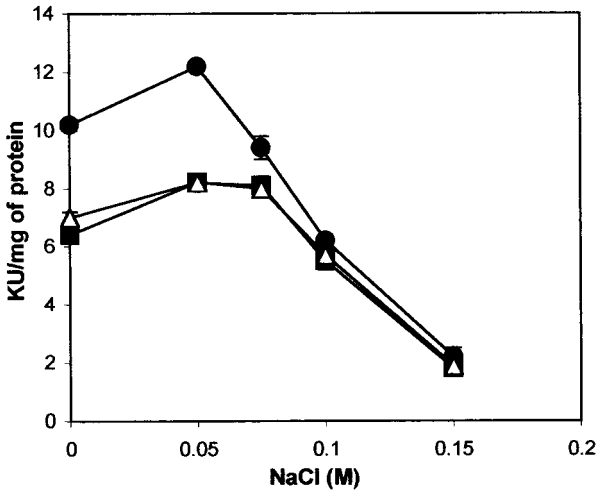

FIGURE 5: Effect of NaCl on the catalytic activity on yeast RNA of ONC (●), (C87S, des104)-ONC (■), and (C87S, des103−104)-ONC (△). All assays were performed in 0.05 M sodium acetate (pH 5.5) in the presence of the indicated NaCl concentration. Standard errors are shown only when they are larger than the symbols.

effect on ONC resistance to proteolysis. The three variants lacking the C-terminal disulfide bridge are completely digested in less than 30 min (Figure 4).

Catalytic Activity. The RNase activity of (C87S, des104)-ONC and (C87S, des103−104)-ONC was assayed on yeast RNA in 50 mM sodium acetate (pH 5.5) in the presence of increasing concentrations of NaCl (see Figure 5). The data indicate that the two mutants have almost the same catalytic activity, and that they are slightly less active than ONC at low ionic strengths.

The catalytic activity of Met(−1)-ONC was assayed only at 0.05 and 0.1 M NaCl. Under these conditions, the protein is ∼40- and ∼90-fold less active than ONC, respectively. This result was already reported by Youle and co-workers (*5*), and was attributed to the loss of the H-bond between Pyr1 and Lys9.

Antitumor Activity. The antitumor activity of ONC, Met-(−1)-ONC, (C87S, des104)-ONC, and (C87S, des103−104)-ONC was assayed on two different malignant cell lines, SVT2 fibroblasts, extensively used in the case of other ribonucleases (*25*−*27*), and K562 erythroleukemic cells, used in the case of recombinant onconase. On both cell lines, ONC, (C87S, des104)-ONC, and (C87S, des103−104)-ONC exhibited identical cytotoxic activity (see Figure 6), with an IC_{50} of ∼25−40 μg/mL. This finding indicates that the removal of the C-terminal disulfide bond has no effect on the antitumor activity of ONC.

Met(−1)-ONC, as previously reported (*5*), has no cytotoxic activity at the protein concentrations that were tested (see Figure 6).

DISCUSSION

The data reported in this paper shed light on the role of N- and C-terminal regions in the stability of ONC. DSC and GuHCl-induced denaturation data, as well as proteolysis experiments, clearly indicate that the two blocks at ONC chain termini, i.e., the pyroglutamyl residue and the disulfide bridge, at the N- and C-terminus, respectively, are responsible for the unusual stability of ONC. On the other hand, the

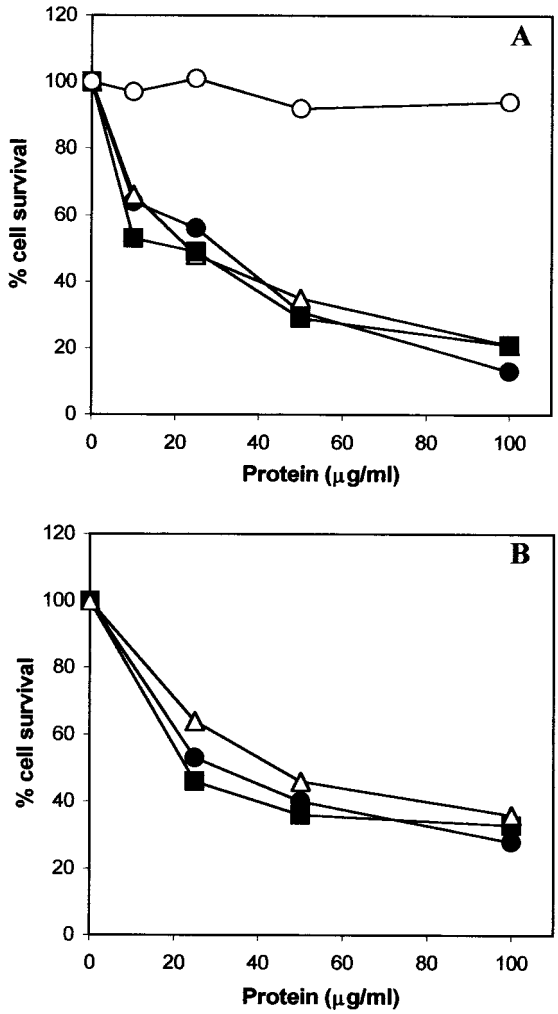

FIGURE 6: Dose−response curves of (A) malignant fibroblasts (SVT2) and (B) human chronic myelogenous leukemia cells (K562) grown in the presence of ONC (●), Met(−1)-ONC (○), (C87S, des104)-ONC (△), and (C87S, des103−104)-ONC (■).

reduced stability of the ONC mutants does not greatly influence either their catalytic or antitumor activity.

It is also evident that the two blocks do not play the same quantitative role in determining the stability of ONC. In fact, the effect of the removal of the cyclized residue at the N-terminus either on the denaturation temperature or on the GuHCl denaturing concentration accounts for ∼10−20% of the total effect measured when the C-terminal disulfide is also removed (Tables 1 and 2). A possible explanation can be found in the three-dimensional structure of ONC.

The crystal structure of Met(−1)-ONC (*5*) shows that helix α1 starts at residue Gln1 instead of residue Trp3 of wild-type ONC (*2*) and that the side chain of Gln1 is no longer H-bonded to Lys9 and Val96 (Figure 1). However, this H-bond loss may be partially counterbalanced by the extra H-bonds gained in the formation of the longer helix α1. This would explain the, albeit modest, contribution of the pyroglutamyl moiety to ONC stability.

On the other hand, the removal of the C-terminal Cys87−Cys104 disulfide bridge causes a decrease in the denaturation temperature of ∼19 °C.

Recently, Raines and co-workers (*28*) replaced the half-cysteines at positions 87 and 104 of ONC with alanine residues, and determined that the variant (C87A/C104A)-

ONC has a T_d of 62 °C at pH 6.0. This result, although in line with the data presented here, would indicate a greater destabilization caused by the double mutation (C87A/C104A) with respect to that induced by the C87S replacement together with the removal of residue 103 and/or 104. In fact, mutants (C87S, des104)-ONC and (C87S, des103−104)-ONC have T_ds of 70.2 and 69.3 °C, respectively, at pH 6.0 in 100 mM MES buffer. These differences may well be attributed to the fact that residue C104 of ONC is highly accessible to solvent and is located at the end of a short tail that is anchored to the body of the molecule only by the terminal disulfide (Figure 1). In the C87A/C104A mutant, this terminal tail, in the absence of any covalent link, would be mobile, thus exposing the two alanine residues to the solvent and invading the adjacent active site cleft, contributing to both the reduced stability and activity. On the other hand, the deletion of the terminal tail and the C87S mutation in (C87S, des104)- and (C87S, des103−104)-ONC could reduce the disorder of the C-terminal end and/or the area of nonpolar surface exposed to the solvent, thus avoiding, at least partially, the destabilizing effect.

As for the effect of the modifications at the C-terminal end on the catalysis, our data would indicate a poor effect on the catalytic activity of the mutants (Figure 5). However, a slight decrease in catalytic activity of both mutants at low ionic strength was measured.

Inspection of structural models for the two mutants indicates that the new C-terminal carboxylates could be closer to the active site cleft with respect to ONC, and this could interfere with the proper docking of the negatively charged substrate because of steric hindrance or charge repulsion. Another hypothesis for the lower activity of the mutants at low ionic strengths could be that the C-terminal carboxylate group plays a role in ONC catalysis. In RNase A, the carboxylate group of Asp121 has a crucial role in catalysis. It has been proposed that the Asp121 side chain stabilizes the catalytically productive conformation of His119 by means of electrostatic attractions between the carboxylate group and the positively charged imidazole ring (*29*, *30*). Asp121 corresponds to Val99 in ONC sequence, and the C-terminal carboxylate is close to Val99 and ∼8 Å from the His97 (corresponding to His119 in RNase A) side chain in the catalytically productive conformation. Although such a distance is usually considered too long for a strong electrostatic interaction in water, it should be taken into account that the aliphatic side chain of Val99 is interposed exactly between the C-terminal carboxylate and the imidazole ring. This could lower the local dielectric constant, thus strengthening the electrostatic interactions. Obviously, this interaction is not as effective as that between His119 and Asp121 in RNase A, and this could be one of the bases for ONC low catalytic activity.

On the other hand, the structural models of the two mutants indicate that the new C-terminal carboxylates could be more distant from His97 than that of native ONC, thus weakening their stabilizing interaction. This could be the basis for the lower activity observed at low ionic strengths. Moreover, as the contribution of this electrostatic interaction should decrease when the ionic strength is increased due to shielding effects, the difference in activity between ONC and the two variant forms should be abolished at high NaCl concentrations, as observed.

As for the antitumor activity of the mutants lacking the C-terminal disulfide bridge, our data indicate that it may not be required for the antitumor action of the protein. However, it should be noted that mutant (C87A/C104A)-ONC has an antitumor activity 10 times lower than that of ONC on K562 cells (*28*). This could be due to the low catalytic activity of the mutant (C87A/C104A)-ONC, whereas our C-terminal mutants are as active as native ONC at physiological ionic strengths. Indeed, it has been demonstrated that ribonuclease activity is essential for the antitumor activity of ONC (*4*, *31*).

Thus, our results would indicate that the C-terminal C87−C104 disulfide bridge makes a large contribution to ONC conformational stability, but not to its biological properties. Therefore, the suggestion that antitumor activity and protein stability are directly correlated, at least for in vitro assays on cell cultures, is not supported by the data presented here.

On the other hand, the modification at the N-terminus has a crucial effect on the antitumor activity (*5*). This might be due to the role of the cyclized residue Pyr1, which proved to be essential for both ribonuclease and antitumor activities (*5*). This hypothesis is reinforced by the finding that the mutant Met(−1)-(Q1S)-ONC has catalytic and antitumor activities even lower than those of ONC (*32*), and that a chimeric ONC, including the N-terminus of human eosinophil-derived neurotoxin, exhibits ribonuclease activity and acts as an efficient toxin in cellular assays (*33*).

As for the biological significance of the interplay between structural stability, catalytic activity, and biological activity in ONC, we should remember that the stability of the protein, resistance to proteases in particular, might play a crucial role in the use of the protein as an antitumor drug in vivo. However, an excessive resistance to proteolysis could also be the cause of ONC accumulation in kidney (*8*) and renal toxicity (*9*). Thus, fine-tuning of ONC resistance to proteases could be a pathway toward the production of an improved antitumor drug.

ACKNOWLEDGMENT

We are indebted to Dr. Giuseppe D'Alessio (Department of Biological Chemistry, University of Naples Federico II) for helpful discussions and for critically reading the manuscript. We also thank Dr. Antimo Di Maro for the determination of the N-terminal sequence of the proteins.

REFERENCES

1. Ardelt, W., Mikulski, S. M., and Shogen, K. (1991) *J. Biol. Chem. 266*, 245−251.
2. Mosimann, S. C., Ardelt, W., and James, M. N. (1994) *J. Mol. Biol. 236*, 1141−1153.
3. Youle, R. J., and D'Alessio, G. (1997) in *Ribonucleases. Structures and Function* (D'Alessio, G., and Riordan, J. F., Eds.) pp 491−514, Academic Press, San Diego.
4. Wu, Y., Mikulski, S. M., Ardelt, W., Rybak, S. M., and Youle, R. J. (1993) *J. Biol. Chem. 268*, 10686−10693.
5. Boix, E., Wu, Y., Vasandani, V. M., Saxena, S. K., Ardelt, W., Ladner, J., and Youle, R. J. (1996) *J. Mol. Biol. 257*, 992−1007.
6. Juan, G., Ardelt, B., Li, X., Mikulski, S. M., Shogen, K., Ardelt, W., Mittelman, A., and Darzynkiewicz, Z. (1998) *Leukemia 12*, 1241−1248.

7. Notomista, E., Catanzano, F., Graziano, G., Dal Piaz, F., Barone, G., D'Alessio, G., and Di Donato, A. (2000) *Biochemistry 39*, 8711−8718.
8. Vasandani, V. M., Burris, J. A., and Sung, C. (1999) *Cancer Chemother. Pharmacol. 44*, 164−169.
9. Vasandani, V. M., Wu, Y. N., Mikulski, S. M., Youle, R. J., and Sung, C. (1996) *Cancer Res. 56*, 4180−4186.
10. Sambrook, J., Fritsch, E. F., and Maniatis, T. (1989) *Molecular Cloning. A Laboratory Manual*, 2nd ed., Cold Spring Harbor Laboratory Press, Plainview, NY.
11. Sanger, F., Nicklen, S., and Coulson, A. R. (1977) *Proc. Natl. Acad. Sci. U.S.A. 76*, 5653−5467.
12. Kunkel, T. A. (1987) *Proc. Natl. Acad. Sci. U.S.A. 82*, 488−492.
13. Notomista, E., Cafaro, V., Fusiello, R., Bracale, A., D'Alessio, G., and Di Donato, A. (1999) *FEBS Lett. 463*, 211−215.
14. Blank, A., Sugiyama, R. H., and Dekker, C. A. (1982) *Anal. Biochem. 120*, 267−275.
15. Freire, E. (1994) *Methods Enzymol. 240*, 502−530.
16. Privalov, P. L. (1979) *Adv. Protein Chem. 33*, 167−241.
17. Zhou, Y., Hall, C. K., and Karplus, M. (1999) *Protein Sci. 8*, 1064−1074.
18. Santoro, M. M., and Bolen, W. (1988) *Biochemistry 27*, 8063−8068.
19. Schagger, H., and von Jagow, G. (1987) *Anal. Biochem. 166*, 368−379.
20. Peitsch, M. C., and Guex, N. (1997) *Electrophoresis 18*, 2714−2723.
21. Laemmli, U. K. (1970) *Nature 227*, 680−685.
22. Kunitz, M. (1946) *J. Biol. Chem. 164*, 563−568.
23. Catanzano, F., Graziano, G., Capasso, S., and Barone, G. (1997) *Protein Sci. 6*, 1682−1693.
24. Pace, C. N., Grimsley, G. R., Thomas, S. T., and Makhatsdze, G. I. (1999) *Protein Sci. 8*, 1500−1504.
25. Mastronicola, M. R., Piccoli, R., and D'Alessio, G. (1995) *Eur. J. Biochem. 230*, 242−249.
26. Di Donato, A., Cafaro, V., Romeo, I., and D'Alessio, G. (1995) *Protein Sci. 4*, 1470−1477.
27. Di Donato, A., Cafaro, V., and D'Alessio, G. (1994) *J. Biol. Chem. 269*, 17394−17396.
28. Leland, P. A., Staniszewski, K. E., Kim, B. M., and Raines, R. T. (2000) *FEBS Lett. 477*, 203−207.
29. Quirk, D. J., Park, C., Thompson, J. E., and Raines, R. T. (1998) *Biochemistry 37*, 17958−17964.
30. Schultz, L. W., Quirk, D. J., and Raines, R. T. (1998) *Biochemistry 37*, 8886−8898.
31. Newton, D. L., Walbridge, S., Mikulski, S. M., Ardelt, W., Shogen, K., Ackerman, S. J., Rybak, S. M., and Youle, R. J. (1994) *J. Neurosci. 14*, 538−544.
32. Newton, D. L., Boque, L., Wlodawer, A., Huang, C. Y., and Rybak, S. M. (1998) *Biochemistry 37*, 5173−5183.
33. Newton, D. L., Xue, Y., Boqué, L., Wlodawer, A., Kung, H. F., and Rybak, S. M. (1997) *Protein Eng. 10*, 463−470.

BI010741S